ISSN 1674-1056
http://cpb.iphy.ac.cn
http://iopscience.iop.org/cpb
中国物理 B
Chinese Physics
中国物理 Chinese Physics B

Helium-hydrogen synergistic effects on swelling in *in-situ* multiple-ion beams irradiated steels

Haocheng Liu(刘昊成), Jia Huang(黄嘉), Liuxuan Cao(曹留煊), Yue Su(苏悦), Zhiying Gao(高智颖), Pengfei Ma(马鹏飞), Songqin Xia(夏松钦), Wei Ge(葛伟), Qingyuan Liu(刘清元), Shuang Zhao(赵双), Yugang Wang(王宇钢), Jinchi Huang(黄金池), Zhehui Zhou(周哲辉), Pengfei Zheng(郑鹏飞), and Chenxu Wang(王晨旭)

Citation: Chin. Phys. B, 2021, 30 (**8**): 086106. DOI: 10.1088/1674-1056/abfcca
Journal homepage: http://cpb.iphy.ac.cn; http://iopscience.iop.org/cpb

What follows is a list of articles you may be interested in

Evolution of helium bubbles in nickel-based alloy by post-implantation annealing

Rui Zhu(朱睿), Qin Zhou(周钦), Li Shi(史力), Li-Bin Sun(孙立斌), Xin-Xin Wu(吴莘馨), Sha-Sha Lv(吕沙沙), and Zheng-Cao Li(李正操)

Chin. Phys. B, 2021, 30 (**8**): 086102. DOI: 10.1088/1674-1056/ac0783

Structural modulation and physical properties of cobalt-doped layered $La_2M_5As_3O_2$ (M= Cu, Ni) compounds

Lei Yang(杨蕾), Yan-Peng Song(宋艳鹏), Jun-Jie Wang(王俊杰), Xu Chen(陈旭), Hui-Jing Du(杜会静), and Jian-Gang Guo(郭建刚)

Chin. Phys. B, 2021, 30 (**7**): 076106. DOI: 10.1088/1674-1056/abf349

Comparison of helium bubble formation in F82H, ODS, SIMP and T91 steels irradiated by Fe and He ions simultaneously

Bingsheng Li(李炳生), Zhen Yang(杨振), Shuai Xu(徐帅), Kongfang Wei (魏孔芳), Zhiguang Wang(王志光), Tielong Shen(申铁龙), Tongmin Zhang(张桐民), and Qing Liao(廖庆)

Chin. Phys. B, 2021, 30 (**3**): 036102. DOI: 10.1088/1674-1056/abc2b4

Extended damage range of $(Al_{0.3}Cr_{0.2}Fe_{0.2}Ni_{0.3})_3O_4$ high entropy oxide films induced by surface irradiation

Jian-Cong Zhang(张健聪), Sen Sun(孙森), Zhao-Ming Yang(杨朝明), Nan Qiu(裘南), Yuan Wang(汪渊)

Chin. Phys. B, 2020, 29 (**6**): 066104. DOI: 10.1088/1674-1056/ab8374

Theoretical derivation of the crystallographic parameters of polytypes of long-period stacking ordered structures with the period of 13 and 14 in hexagonal close-packed system

Li Ye(叶礼), Dong-Shan Zhao(赵东山), Yuan-Lin Zhuang(庄园林), Shuang-Feng Jia(贾双凤), Jia-Ping Zhou(周嘉萍), Jia-Nian Gui(桂嘉年), Jian-Bo Wang(王建波)

Chin. Phys. B, 2018, 27 (**9**): 096102. DOI: 10.1088/1674-1056/27/9/096102

SPECIAL TOPIC — Ion beam modification of materials and applications

Helium–hydrogen synergistic effects on swelling in *in-situ* multiple-ion beams irradiated steels*

Haocheng Liu(刘昊成)[1], Jia Huang(黄嘉)[1], Liuxuan Cao(曹留煊)[2], Yue Su(苏悦)[1], Zhiying Gao(高智颖)[1], Pengfei Ma(马鹏飞)[2], Songqin Xia(夏松钦)[1], Wei Ge(葛伟)[1], Qingyuan Liu(刘清元)[1], Shuang Zhao(赵双)[1], Yugang Wang(王宇钢)[1], Jinchi Huang(黄金池)[2], Zhehui Zhou(周哲辉)[2], Pengfei Zheng(郑鹏飞)[3], and Chenxu Wang(王晨旭)[1,†]

[1] *State Key Laboratory of Nuclear Physics and Technology, Peking University, Beijing* 100871, *China*
[2] *College of Energy, Xiamen University, Xiamen* 361102, *China*
[3] *Southwestern Institute of Physics, China National Nuclear Corporation, Chengdu* 610041, *China*

(Received 17 March 2021; revised manuscript received 24 April 2021; accepted manuscript online 29 April 2021)

The development of reliable fusion energy is one of the most important challenges in this century. The accelerated degradation of structural materials in fusion reactors caused by neutron irradiation would cause severe problems. Due to the lack of suitable fusion neutron testing facilities, we have to rely on ion irradiation experiments to test candidate materials in fusion reactors. Moreover, fusion neutron irradiation effects are accompanied by the simultaneous transmutation production of helium and hydrogen. One important method to study the He–H synergistic effects in materials is multiple simultaneous ion beams (MSIB) irradiation that has been studied for decades. To date, there is no convincing conclusion on these He–H synergistic effects among these experiments. Recently, a multiple ion beam *in-situ* transmission electron microscopy (TEM) analysis facility was developed in Xiamen University (XIAMEN facility), which is the first triple beam system and the only in-running *in-situ* irradiation facility with TEM in China. In this work, we conducted the first high-temperature triple simultaneous ion beams irradiation experiment with TEM observation using the XIAMEN facility. The responses to *in-situ* triple-ion beams irradiation in austenitic steel 304L SS and ferritic/martensitic steel CLF-1 were studied and compared with the results in dual- and single-ion beam(s) irradiated steels. Synergistic effects were observed in MSIB irradiated steels. Helium was found to be critical for cavity formation, while hydrogen has strong synergistic effect on increasing swelling.

Keywords: helium–hydrogen synergistic effect, multiple ion beams, structural material, swelling

PACS: 61.80.Jh, 61.72.–y, 41.75.Ak, 28.52.–s **DOI:** 10.1088/1674-1056/abfcca

1. Introduction

Nuclear energy is one of the most important options for reliable, environmentally sustainable and economical energy,[1] and the development of fusion energy is one of the top challenges. Besides plasma physics and fusion technology issues, the research and development of materials in fusion reactors is critical.[2] A hard neutron spectrum, including 14-MeV neutrons from the deuterium–tritium fusion, in fusion reactors introduces massive defects and results in radiation damages in structural materials.[3] Additionally, a particular concern is the simultaneous transmutation production of helium and hydrogen.[4] The displacement damage and helium accumulation rates in fusion reactors are about one to two orders of magnitude greater than those in present fission reactors, and extra production of hydrogen also influences the radiation effects in materials. The helium and displacement defects promote hydrogen retention in materials and H can couple with them, making the synergistic effect of helium and hydrogen an inevitable problem.[3] It was reported that helium and hydrogen can greatly influence the nucleation and growth behaviors of cavity, enhance void swelling, deteriorate mechanical properties, and then accelerate the failure of structural materials.[5] Therefore, to develop advanced structural materials for fusion systems, the synergistic effects of helium and hydrogen need to be well understood.

Due to the lack of fusion neutron sources and integrated materials testing facilities, previous investigations of He–H synergistic effects were mainly based on several simulation experimental approaches, while its mechanism is still not well understood. One notable experimental technique is multiple ion beams irradiation (heavy ion + He + H), which can simulate the damage process in a relatively short period of time with no residual radioactivity, and can systematically control irradiation conditions (ion species, temperature, dose, dose rate, He/H production rate, *etc.*).[6,7] Multiple simultaneous ion beams (MSIB) irradiations on metals have been conducted in the past few decades, providing us some evidence of the synergistic effect. Wakai *et al.*[8] reported that the void swelling was significantly enhanced by 40 times for F82H, a well-studied RAFM steels, under Fe + He + H triple ion irra-

*Project supported by the National Natural Science Foundation of China (Grant No. 11935004).
†Corresponding author. E-mail: cxwang@pku.edu.cn
© 2021 Chinese Physical Society and IOP Publishing Ltd

diation compared with that under Fe + He dual ion irradiation. This observation has been being used as a typical evidence of the synergistic effect, yet the conclusion is still controversial due to the overestimated damage and gas rate compared to fusion system. In Borodin's experiment,[9] the synergistic effects exhibit apparent complex temperature dependence as the void swelling under tripe beams is enhanced or suppressed relative to Cr + He or Cr + H dual beams with the increase of temperature. However, it was found that the peak swelling temperature of MSIB irradiated steels is about 450 °C–550 °C.[5,10] Besides, Sekimura *et al.*[11] suggested that the concentration of He/H also plays an important role in synergistic effects. They found that the vanadium alloy shows maximum irradiation swelling when the implantation rate of He and H is about 10 appm/dpa. The effect of hydrogen plays a critical role in the synergistic effects. In the work reported by Brimbal,[12] the existence of hydrogen in materials under triple ion irradiation (Fe + He + H) increases the number density of cavities compared to dual beams irradiation (Fe + He). In contrast, the effect of hydrogen on the size of cavities under irradiation is still not clear and strongly dependent on irradiation conditions, such as temperature.[10,13] However, in some cases, increased dose of hydrogen could lead to decrease in swelling in RAFM steel.[14] Therefore, there is no convincing conclusion on the synergistic effects among these experiments. The efforts in theoretical calculations helped to understand the details of the synergistic effects of helium and hydrogen.[3] There exists almost no direct interaction between He and H, while the formation of He–V (vacancy) and He–V–H complex cluster significantly affects the behavior of cavity and the structure of materials. Overall, the comprehensive understanding of He–H synergistic effects and the role of hydrogen needs more experimental observations.

Recently, a multiple ion beam *in-situ* TEM analysis facility was developed in Xiamen University (XIAMEN facility) which is the first triple beam system and the only in-running *in-situ* irradiation facility with TEM in China.[15] This facility consists of a TECNAI G20 F30 TWIN TEM coupled to a 400-kV implanter and a 50-kV hydrogen/helium coaxial ion source. It provides the ability of performing MSIB (heavy ion + He^+ + H_2^+) irradiation and *in-situ* observation. With a Gatan 652 heat holder, the temperature of *in-situ* irradiation can be elevated up to 1000 °C. Moreover, the dose rate of heavy ions and/or He/H ions can be changed by more than two orders of magnitude, making it a unique and powerful facility which provides an excellent way of studying the He–H synergistic effects in structural materials.

Steels are primary structural materials in nuclear systems. Austenitic stainless steels (ASS) are widely used in reactor structural components for their outstanding corrosion resistance, ductility and economic efficiency.[2] Additionally, reduced activation ferritic-martensitic (RAFM) steels are potential candidate materials for fusion reactors, due to their good thermomechanical properties, good radiation resistance and capability of large-scale industrial fabrication.[16] Compared to F/M steels, ASSs have higher creep resistance, but exhibit poor void swelling resistance.[17] In contrast, RAFM steels exhibit poor long-term thermal aging behavior, significant radiation embrittlement and void swelling under neutron irradiation.[16] The response of these steels to MSIB irradiation is critical in the research of structural materials in fusion reactors.

In this work, using the XIAMEN facility, we conducted the first high-temperature triple simultaneous ion beams irradiation experiment with TEM observation on this facility. The responses to MSIB irradiation of conventional 304L ASS (304L SS) and an advanced RAFM steel (CLF-1)[18] were studied.

2. Materials and methods

The commercially available conventional austenitic steel 304L SS has an average grain size of ∼ 30 μm and is austenitic throughout. The advanced RAFM steel CLF-1 was developed by the Southwestern Institute of Physics of China. The manufacture of CLF-1 was described by Du *et al.*[18] Specimens for the *in-situ* irradiation and TEM observations tests were prepared by focused ion beam (FIB). To calculate the volume swelling of the specimens after irradiation, the thickness of each specimen was determined using electron energy loss spectroscopy (EELS). The average thickness of specimens used in this study is ∼ 70 nm.

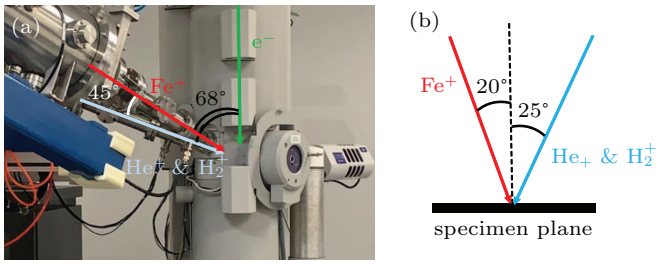


Fig. 1. (a) The coupled TEM and ion implanters in XIAMEN facility. The Fe^+ ion and the He^+ & H_2^+ ion beams both have 68° intersection angles with the electron beam in the TEM, and the angle between the two ion beams is 45°. (b) Schematic diagram of the directions of the incident ion beams on the specimen when irradiating in the TEM.

The geometry of the multi-beam system in the XIAMEN facility is shown in Fig. 1. The two ion beam lines both have 68° intersection angles with the electron beam in the TEM (TECNAI G20 F30), and the angle between the two ion beam lines is 45°. Due to the shape of the specimen holder (Gatan 652 heating holder), the ion beams are blocked by the holder during the observation of the sample using electron beam. Therefore, the specimens were tilted to −68° (α) and 20°

(β) during irradiation, such that simultaneous *in-situ* TEM observation during irradiation can be performed. As shown in Fig. 1(b), the angle between the specimen plane and the heavy ion beam is 20°, and that between the specimen plane and the He & H ion beam is 25°. After irradiation for 15 minutes, the ion beams were cut off and the position of the specimen was reset for TEM observation. In each test, the total irradiation time was 75 minutes, five observations were taken at 20%, 40%, 60%, 80%, and 100% of the total irradiation time (dose).

The 400-keV Fe^+, 30-keV He^+, and 30-keV H_2^+ ions were used for irradiation. The damage profile induced by Fe^+ ion irradiation, the concentrations of He and H in 304L SS are calculated using SRIM-2013 (Stopping Range of Ions in Matter), as shown in Fig. 2. The dpa and the concentration of He & H are calculated by averaging over the effective depth ($\sim$ 70 nm), as indicated by the orange area in Fig. 2. Due to the significant surface effect of a thin specimen and the high diffusion rate of He and H, relatively high He-concentration/dpa and H-concentration/dpa ratios were used. The ion fluxes were set as: $Fe^+ \sim 1.8 \times 10^{12}$ cm^{-2}·s^{-1}, $He^+ \sim 4.3 \times 10^{11}$ cm^{-2}·s^{-1}, and $H_2^+ \sim 2.1 \times 10^{12}$ cm^{-2}·s^{-1}, respectively. The H_2^+ will dissociate into two H^+ ions when it bombards the specimen surface.[19] The ratio between the concentration of He and H and damage in a 70-nm thick specimen is $\sim$ 31 appm/dpa and $\sim$ 340 appm/dpa, respectively, such that the total amount of damage dose and concentration of He and H would be $\sim$ 18.6 dpa, $\sim$ 570-appm He, and $\sim$ 6360-appm H at the highest irradiation fluence. The actual dpa and concentration of He & H were calculated based on the thickness of different specimens measured by EELS. The total displacement damage induced by He and H ion implantations is only $\sim$ 0.14 dpa and thus can be neglected. The irradiation temperature was set as 450 °C. To study the effects of hydrogen and helium, triple-ion beams ($Fe^+ + He^+ + H_2^+$), dual-ion beams ($Fe^+ + He^+$) and single-ion beam (Fe^+) irradiation were conducted using the same irradiation conditions.

The *in-situ* heating by the specimen holder induced significant thermal drift. The vacuum systems of the two ion implanters linked to the TEM also induced strong vibration. As a result, the imaging quality was greatly influenced. Therefore, to identify the cavities during *in-situ* observations, the images were taken with a higher defocus of about -2 μm to get clearer contrast of cavity boundaries. The size and density of cavities in each case were measured and counted manually based on the TEM images. All cavities in a randomly selected region were measured and counted, at least 200 cavities were counted in each case. The total volume of all the cavities measured were taken as the volume expansion of the selected region in each case. The errors of manual measurements were considered in the error bars.

It should be noted that the thickness of a TEM specimen causes a strong surface effect. The free surfaces of the specimen would act as sinks for defects.[20] Modeling study indicated that the surface effect for displacement damage in a specimen thicker than 60 nm would be relatively non-significant.[21] However, He and H exhibit high diffusion rates, the surface effects of He and H would be more significant. Therefore, the quantification of surface effects required further research.

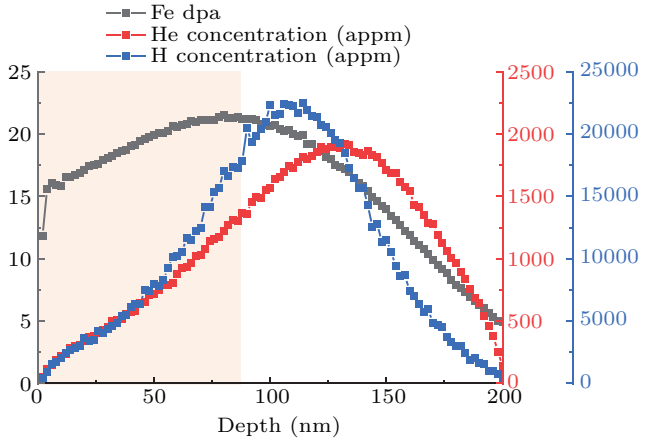


Fig. 2. Damage induced by 400-keV Fe^+ ion irradiation and the concentration of 30-keV He^+ & H_2^+ ions in 304L SS calculated using SRIM-2013. The orange block indicates the approximate effective depth of 70-nm thick specimen.

3. Results

Cross-sectional bright field TEM images of the triple- and dual-ion beams irradiated 304L SS specimens to different doses are shown in Fig. 3. Images at different doses were taken at the same area as in the initial sample. At $\sim$ 7.4 dpa, large cavities appeared in both irradiation conditions. As the dose increases, the amount and the size of these cavities increases. The high-resolution TEM images in Figs. 3(m) and 3(n) showed the co-existing large cavities and normal-sized cavities. The size distributions of cavities in triple- and dual-ion beams irradiated 304L SS are shown in Fig. 5, respectively, in which large cavities are found to be co-existing with small cavities. The size of cavities smaller than 5.5 nm shows approximately Gaussian distribution. At the highest dose, the number density of cavities in triple-ion beams irradiated 304L SS was larger than that in dual-ion beam irradiated 304L SS, as shown in Fig. 6(a). At the highest dose, the number density of large cavities ($>$ 5.5 nm) in triple-ion beams irradiated 304L SS ($\sim 2.4 \times 10^{16}$ cm^{-3}) was also larger than that in dual-ion beams irradiated 304L SS ($\sim 7.2 \times 10^{15}$ cm^{-3}). The contributions of large cavities in the total volume swelling in triple-

and dual-ion beam irradiated 304L SS were 68% and 75%, respectively. As shown in Fig. 3(o), no obvious cavity was found in single-ion beam irradiated 304L SS.

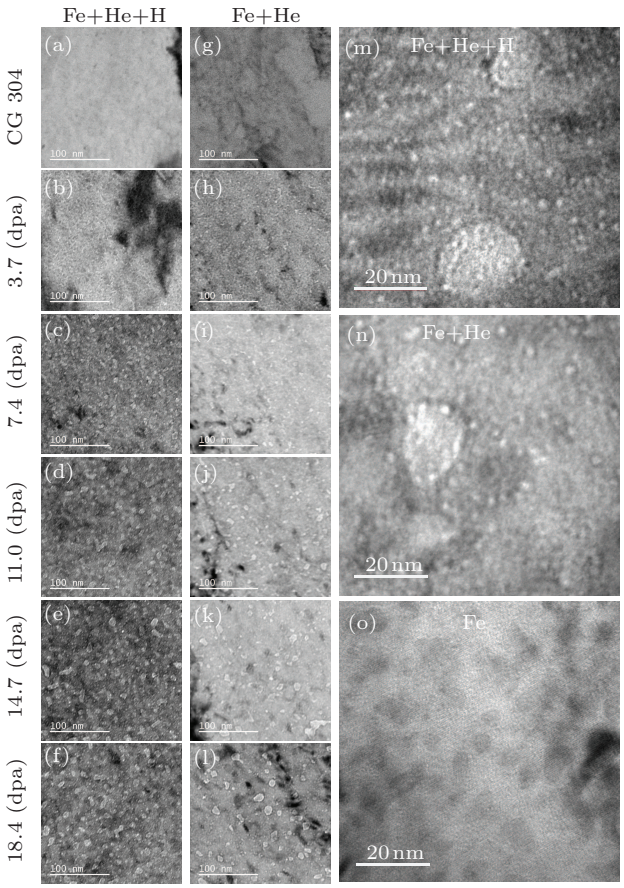


Fig. 3. (a)–(f) The 304L SS sample before and after irradiated by *in-situ* triple-ion beams to different doses. (g)–(l) The 304L SS sample before and after irradiated by *in-situ* dual-ion beams to different doses. (m)–(o) High-resolution TEM images in 304L SS samples after triple-ion beam, dual-ion beam, and single Fe ion irradiation to the highest doses, respectively. In triple- and dual-ion beams irradiated 304L SS, the size and density of cavities increased with dose. In triple- and dual-ion beams irradiated 304L SS, large cavities are found to be co-existing with small cavities. The number densities of small and large cavities in triple-ion beams irradiated 304L SS were both higher than those in dual-ion beams irradiated 304L SS. Triple-ion beams irradiation induced a higher swelling ratio in 304L SS than dual-ion beams. No obvious cavity was found in single Fe ion irradiated 304L SS.

In contrast, cavities in MSIB irradiated CLF-1 showed different structures as shown in Fig. 4. There was also no obvious cavity in single-ion beam irradiated CLF-1 as shown in Fig. 4(o), but no large cavity (> 5.5 nm) was observed in triple- and dual-ion beams irradiated CLF-1. At the highest dose, the number density of cavities in triple-ion beams irradiated CLF-1 was lower than that in dual-ion beam irradiated 304L SS, but the average size of cavities was larger, as shown in Figs. 6(a) and 6(b). The size distributions of cavities in triple- and dual-ion beams irradiated CLF-1 are shown in Fig. 5.

The swelling ratios in 304L SS and CLF-1 irradiated to the highest dose are shown in Fig. 6(c). The austenitic 304L SS exhibits much higher swelling than the ferritic/martensitic CLF-1. The change of swelling ratios at different doses of 304L SS and CLF-1 were shown in Fig. 7.

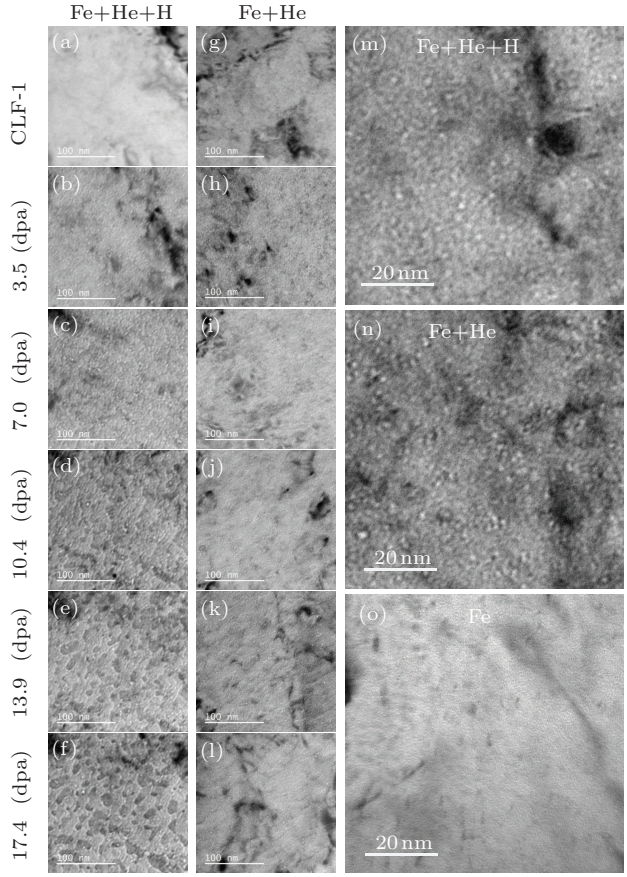


Fig. 4. (a)–(f) The CLF-1 sample before and after irradiated by *in-situ* triple-ion beams to different doses. (g)–(l) The CLF-1 sample before and after irradiated by *in-situ* dual-ion beams to different doses. (m)–(o) High-resolution TEM images in CLF-1 samples after triple-ion beam, dual-ion beam, and single Fe ion irradiation to the highest doses, respectively. In triple- and dual-ion beams irradiated CLF-1, the size and density of cavities increased with dose. The average size of cavities in triple-ion beams irradiated CLF-1 was larger than that in dual-ion beams irradiated CLF-1, but the number density was lower. Triple-ion beams irradiation induced a higher swelling ratio in CLF-1 than dual-ion beams. No obvious cavity was found in single Fe ion irradiated CLF-1.

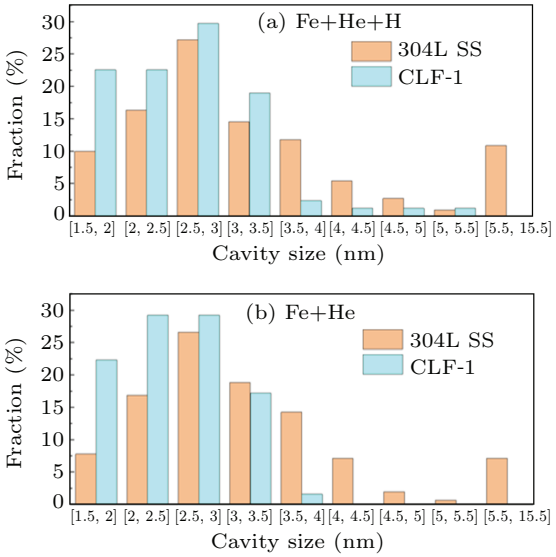


Fig. 5. Size distributions of cavities in (a) triple-ion and (b) dual-ion beams irradiated 304L SS and CLF-1 to the highest dose, respectively.

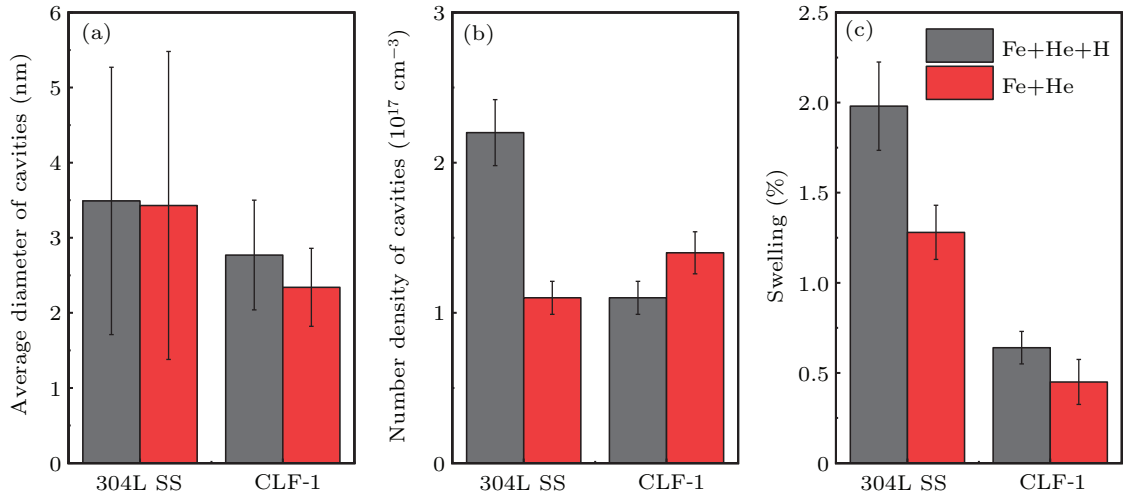


Fig. 6. (a) Average diameters of cavities, (b) number density of cavities, and (c) swelling ratio in 304L SS and CLF-1 after triple- and dual-ion beam irradiation to the highest dose.

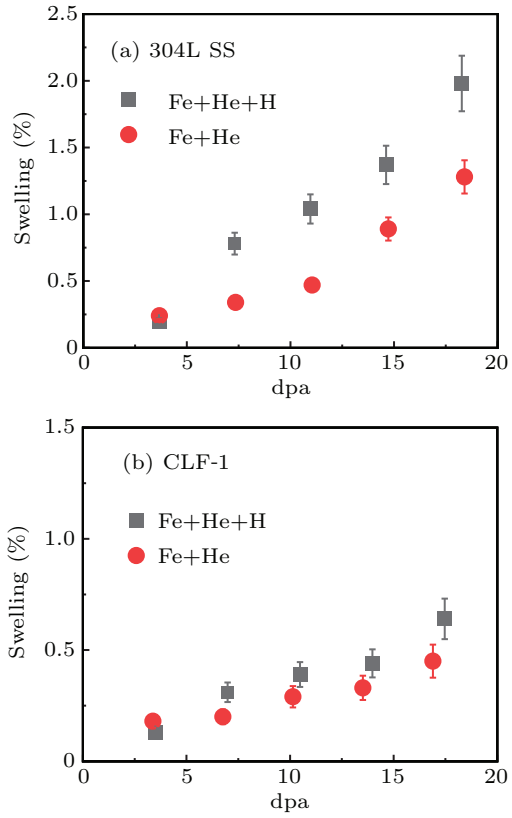


Fig. 7. Change of swelling ratios with dose of triple- and dual-ion beam irradiated (a) 304L SS and (b) CLF-1. Dpa was calculated according to the actual thickness of the sample in each case.

As no obvious cavity was found in single-ion beam irradiated 304L SS and CLF-1, the swelling in single-ion beam irradiated 304L SS and CLF-1 would be treated as 0 and therefore neglected in further discussion on swelling. The swelling ratios in triple- and dual-ion irradiated 304L SS and CLF-1 both increased with dose. At high doses, triple-ion irradiation induced larger swelling in these materials than dual-ion irradiation. The increase in total swelling induced by hydrogen at the highest dose was $\sim 54\%$ in 304L SS and $\sim 42\%$ in CLF-1, indicating the significant effect of hydrogen on swelling.

4. Discussion

Triple- and dual-ion beams irradiation both lead to the formation of cavities in both steels, while the swelling in 304L SS was more significant. It is known that austenitic steels have worse swelling resistance compared to ferritic/martensitic steels.[17] Large cavities were only found in 304L SS, indicating better swelling resistance of RAFM steels than austenitic steels.

Helium was found to be critical in the formation of cavities. As shown in Figs. 3 and 4, single Fe ion irradiation induced no obvious cavity, while massive cavities were found in dual-ion (Fe + He) beams irradiated specimens. Helium can easily bond to a vacancy forming He–V pairs, or bond to another He atom forming di-He clusters, promoting the formation of cavities.[22,23] On the other hand, the accumulation of He atoms and vacancies results in the formation of He bubbles. He bubbles with a critical diameter of several nanometers remain stable as spherical bubbles.[24] He bubbles further act as sinks for vacancies, capturing vacancies and growing without bound to form voids.[25,26] In dual-ion beams irradiation, the combination of displacement damage induced by heavy ions and the implanted He atoms would result in increase of swelling.[5,27]

In contrast, single hydrogen ion beam irradiation or heavy ion + H dual-ion beams irradiation causes no significant swelling.[5] The solution energy of hydrogen is much lower than that of helium in iron,[28,29] leading to a higher solubility of hydrogen in comparison with helium. However, hydrogen is also a fast diffuser in metals. Hydrogen could easily migrate out of the lattice, especially at elevated temperatures.[30] In triple-ion beams irradiated F82H, hydrogen could be detected in specimens irradiated at room temperature, but no hydrogen could be found in the specimens irradiated at 470 °C, indicating the high mobility of hydrogen at high temperature.[10] Hydrogen can be readily trapped in vacancies and form H–V

complex, yet the hydrogen atoms can hardly form bound state with other H atoms.[31,32] Saturation of the hydrogen retention would be reached at a rather low irradiation dose.[33] Therefore, the existence of hydrogen atoms does not significantly influence the swelling under single or dual ion irradiation.

However, hydrogen may interact with helium under triple ion beam irradiation in multiple ways. Helium bubbles were found to be strong traps for hydrogen atoms.[34] He bubbles can also prevent hydrogen atoms from trapping by vacancies and therefore most hydrogen would be trapped by He bubbles.[33] Atomistic simulation study indicated that the structure of He–H–V clusters appeared to be a core of helium surrounded by a shell of hydrogen atoms which are attracted to the bubble's free surface.[4] Molecular dynamics simulation has also found that hydrogen tends to diffuse to the outer layer of He bubbles and a large amount of hydrogen would be bound within the first 1–2 layer of the matrix surrounding the bubble.[35] Therefore, He bubbles significantly enhanced the hydrogen retention in metals. Meanwhile, hydrogen atoms are able to assist bubble nucleation and helium diffusion and further stabilize He bubbles. Only a weak van der Walls bond could be formed between He and H, yet H can increase the binding of He and vacancies.[4]

According to atomistic simulation, hydrogen can be easily released from the He–H–V complex.[36] The diffused H atoms could be captured by another He bubble and again participate in the stabilization of the bubble, resulting in a more stabilized He bubble.[37] The diffusion of He atoms or He–V clusters can be also enhanced by hydrogen.[14] At proper temperatures, such as 450 °C in this work, the enhanced diffusion of He atoms results in the growth of He bubbles. However, at higher temperatures, the bubble size decreases and the bubble density increases due to the enhanced diffusion, possibly hindering swelling.[3] Therefore, at 450 °C, hydrogen implantation exhibits synergistic effect on swelling in steels as proved by our experimental results.

In triple- and dual-ion beams irradiated 304L SS, large cavities are found to be co-existing with small cavities. A similar cavity structure has also been reported in multi-ion beam irradiated metals.[8,27,38] The evolution of swelling with irradiation damage can be divided into three regimes:[39] the incubation regime where nucleation is dominant; the transition regime where new cavities nucleate while existing cavities grow; and the regime dominated by growth where nucleation of small cavities is suppressed by the sink strength of large cavities. The size distribution of cavities in triple- and dual-ion beams irradiated 304L SS indicated that the evolution of cavities was going through the transition regime and not yet saturated. The total swelling could still increase with further increasing irradiation dose. However, no large cavity was found in CLF-1. Experimental study has found that compared to the helium bubbles in ferritic/martensitic steel which mainly located on dislocations, the uniformly distributed helium bubbles in austenitic steels could retain a greater quantity of hydrogen.[40] Therefore, the synergistic effect of hydrogen in austenitic 304L SS should be more significant than that in ferritic/martensitic CLF-1. On the other hand, cavity structures in MSIB irradiated steels are strongly associated with temperature.[5] Another possible explanation of the different cavity structures in 304L SS and CLF-1 would be the different temperature dependence of cavity evolutions in austenitic and ferritic/martensitic steels.

5. Conclusions

In this work, we studied the responses to *in-situ* MSIB irradiation in 304L SS and CLF-1 using the XIAMEN facility. This was the first high-temperature simultaneous triple ion beams irradiation experiment with TEM observation using this facility. Triple-, dual-, and single-ion irradiation experiments were conducted. Helium is found to be critical for cavity formation. The synergistic effect of helium and hydrogen was observed in the experiments, as triple-ion irradiation induced significant increase in swelling than dual-ion irradiation at 450 °C. The ferritic/martensitic steel CLF-1 showed significantly less swelling than the austenitic steel 304L SS in response to MSIB irradiation. The synergistic effect of hydrogen in CLF-1 was also much less significant than in 304L SS. These results indicated that compared to austenitic steels, ferritic/martensitic steels show better radiation resistance in fusion irradiation environment.

References

[1] Zinkle S J and Snead L L 2014 *Ann. Rev. Mater. Res.* **44** 241
[2] Zinkle S J, Möslang A, Muroga T and Tanigawa H 2013 *Nucl. Fusion* **53** 104024
[3] Marian J, Hoang T, Fluss M and Hsiung L L 2015 *J. Nucl. Mater.* **462** 409
[4] Hayward E and Deo C 2012 *J. Phys.: Condens. Matter* **24** 265402
[5] Tanaka T, Oka K, Ohnuki S, Yamashita S, Suda T, Watanabe S and Wakai E 2004 *J. Nucl. Mater.* **329–333** 294
[6] Zinkle S J and Snead L L 2018 *Scripta Materialia* **143** 154
[7] Was G S 2015 *J. Mater. Res.* **30** 1158
[8] Wakai E, Sawai T, Furuya K, Naito A, Aruga T, Kikuchi K, Yamashita S, Ohnuki S, Yamamoto S, Naramoto H and Jistukawa S 2002 *J. Nucl. Mater.* **307–311** 278
[9] Borodin O V, Bryk V V, Kalchenko A S, Melnichenko V V, Voyevodin V N and Garner F A 2013 *J. Nucl. Mater.* **442** S817
[10] Wakai E, Kikuchi K, Yamamoto S, Aruga T, Ando M, Tanigawa H, Taguchi T, Sawai T, Oka K and Ohnuki S 2003 *J. Nucl. Mater.* **318** 267
[11] Sekimura N, Iwai T, Arai Y, Yonamine S, Naito A, Miwa Y and Hamada S 2000 *J. Nucl. Mater.* **275** 5
[12] Brimbal D, Beck L, Troeber O, Gaganidze E, Trocellier P, Aktaa J and Lindau R 2015 *J. Nucl. Mater.* **465** 236
[13] Wakai E, Ando M, Sawai T, Kikuchi K, Furuya K, Sato M, Oka K, Ohnuki S, Tomita H, Tomita T, Kato Y and Takada F 2006 *J. Nucl. Mater.* **356** 95
[14] Chen J, Guo L, Luo F, Li T, Ren Y and Suo J 2014 *Fusion Sci. Technol.* **66** issue 2

[15] Huang M, Li Y, Ran G, Yang Z and Wang P 2020 *J. Nucl. Mater.* **538** 152240
[16] Zinkle S J, Boutard J L, Hoelzer D T, Kimura A, Lindau R, Odette G R, Rieth M, Tan L and Tanigawa H 2017 *Nucl. Fusion* **57** 092005
[17] Garner F A, Toloczko M B and Sencer B H 2000 *J. Nucl. Mater.* **276** 123
[18] Liao H, Wang X, Yang G, Feng Y, Wang P and Feng K 2019 *Fusion Engineering and Design* **147** 111235
[19] Kupriiyanova Y E, Bryk V V, Borodin O V, Kalchenko A S, Voyevodin V N, Tolstolutskaya G D and Garner F A 2016 *J. Nucl. Mater.* **468** 264
[20] Chen D, Murakami K, Abe H, Li Z and Sekimura N 2019 *Acta Materialia* **163** 78
[21] Xu D, Wirth B D, Li M and Kirk M A 2012 *Acta Materialia* **60** 4286
[22] Trinkaus H and Singh B N 2003 *J. Nucl. Mater.* **323** 229
[23] Gao F, Heinisch H L and Kurtz R J 2007 *J. Nucl. Mater.* **367–370** 446
[24] Odette G R and Hoelzer D T 2010 *JOM* **62** 84
[25] Mansur L K and Coghlan W A 1983 *J. Nucl. Mater.* **119** 1
[26] Stoller R E and Odette G R 1985 *J. Nucl. Mater.* **131** 118
[27] Taller S and Was G S 2020 *Acta Materialia* **198** 47
[28] Kholtobina A S, Pippan R, Romaner L, Scheiber D, Ecker W and Razumovskiy V I 2020 *Materials* **13** 2288
[29] Li L, Shi J, Peng L, Jiang W and Qian G 2019 *Comput. Mater. Sci.* **170** 109192
[30] Klueh R L 2005 *Int. Mater. Rev.* **50** 287
[31] Jung P, Liu C and Chen J 2001 *J. Nucl. Mater.* **296** 165
[32] Henriksson K O E, Nordlund K, Krasheninnikov A and Keinonen J 2005 *Appl. Phys. Lett.* **87** 163113
[33] Kobayashi M, Shimada M, Hatano Y, Oda T, Merrill B, Oya Y and Okuno K 2013 *Fusion Engineering and Design* **88** 1749
[34] Lee S R, Myers S M and Spulak R G 1989 *J. Appl. Phys.* **66** 1137
[35] Juslin N and Wirth B D 2013 *J. Nucl. Mater.* **438** S1221
[36] Kirsanov V V, Musina M V and Rybin V V 1992 *J. Nucl. Mater.* **191–194** 1318
[37] Kim S, Jin H H, Kim H, Heo J, Cho S Y, Shin C, Moon J and Lee C H 2020 *J. Korean Phys. Soc.* **77** 32
[38] Taller S, Jiao Z, Field K and Was G S 2019 *J. Nucl. Mater.* **527** 151831
[39] Getto E, Vancoevering G and Was G S 2017 *J. Nucl. Mater.* **484** 193
[40] Binyukova S Yu, Chernov I I, Kalin B A and Swe T 2007 *J. Nucl. Mater.* **367–370** 500